J. Water Environ. Nanotechnol., 8(1): 34-40 Winter 2023

ORIGINAL RESEARCH PAPER

The Al_2O_3-monolayer sensitivity towards NH_3 and PH_3 molecule: A DFT Study

Syed Reyaz Hasan[1], Zaheer Abbas[2], Md. Shahzad Khan[3,*]

[1] *Department of Physics, D. A. V. P. G. College, Siwan, India*
[2] *Department of Science and Humanities, Government Engineering College, Jehanabad, Bihar, India*
[3] *Department of Physics, Z. A. Islamia P. G. College, Siwan, Bihar, India*

Received: 2022-09-29 Accepted: 2022-12-07 Published: 2023-02-11

ABSTRACT

The recent theoretical investigation has advocated the Al_2O_3 monolayer as a stable atomic configuration. This work deals with the interaction of NH_3 and PH_3 towards this monolayer configuration. Structural and electronic investigation suggests a strong affinity of the monolayer towards the NH_3 and PH_3 molecules. PDOS analysis reveals hybridization between the molecular orbital of NH_3/PH_3 and Al_2O_3-monolayer. The electronic energy bandgap of the Al_2O_3 monolayer gets reduced by 0.26eV and 0.21eV, respectively on NH_3 and PH_3 adsorption. In the band structure analysis of the Al_2O_3-monolayer, the energy band dispersion got flattened after the toxic molecular gas (NH_3/PH_3) adsorption, suggesting strong sensitivity towards the toxicants. Mulliken population analysis witnessed a robust amount of charge transferred from the toxic molecules to the Al_2O_3-nanosheet. A competency in electrical conductivity and energy-band gap flattening of the NH_3/PH_3-Al_2O_3 configurations is an interesting outcome of the present work. All these findings suggest strong sensitivity of the 2D-monolayer for NH_3/PH_3.

Keywords: DFT, Band structure, Density of State, Mulliken Population Analysis

How to cite this article
Shahzad Khan M. D., Abbas Z., Hasan S. R., The Al_2O_3-monolayer sensitivity towards NH_3 and PH_3 molecule: A DFT Study. J. Water Environ. Nanotechnol., 2023; 8(1): 34-40 DOI: 10.22090/jwent.2023.08.004

INTRODUCTION

The discovery of graphene is followed by several other novel 2D nanosheets, like boron nitride, silicene, antimonene, arsenene, germenene, etc [1]. These 2D sheets are widely been explored for having interesting electronic, optical, and transport properties [2-9]. At the same time, realizing the extra degree of chemical and physical freedom provided by the nanosurfaces, several groups have explored different molecules' sensitivity towards it both theoretically and experimentally [10-14]. In the race to find a novel 2D-monolayer, recently, Al_2O_3 nanosheet is predicted and its stability has been confirmed theoretically [15]. Yet the finding is in very infant mode, experimental establishment of the monolayer needs to be investigated. On the other hand, eradicating poisonous gases from the environment is a need of the hour. To accomplish this aim, the scientific communities have worked on a war footing [16-19]. NH_3 and PH_3 are toxic hazardous molecules that cause severe health effects in the human body. The NH_3 is released into the environment during the production of pesticides, plastics, explosives, dyes, and tyles. The NH_3 harms human bodies by interfering with the normal function of the eyes, throat, and skin. It also consequently decreases the concentration level of oxygen in hemoglobin, hence long-time exposure could be the reason for metabolic activities break down [20-21]. Phosphine in the semiconductor industry works as an agent to introduce phosphorus into silicon crystals. PH_3 is used as an insecticide and pesticide for pollen grains [22]. But its excessive presence in the environment leads to abnormalities in human development. PH_3 attacks the central nervous system and lungs which leads to death. The

* Corresponding Author Email: *kshahzad001@gmail.com*

symptom of PH_3 exposure to human health could be nausea, vomiting, abdominal pain, diarrhea, chest pain, etc. The collective observation of the novelty of the Al_2O_3 nanosheet and the demand for poisonous gas sensors, motivate us to explore the sensitivity of Al_2O_3 monolayer towards the ammonia (NH_3) and phosphine (PH_3) molecules using quantum chemical investigation based on density functional theory (DFT). Previous works have shown dangling lone pairs from NH_3 and PH_3 played an important role in their binding with different nanosurfaces [23, 24]. Thus, any electron-deficient region on the Al_2O_3 nanosurface could be the NH_3/PH_3 catcher.

COMPUTATIONAL METHOD

A 2x2 supercell consisting of 20 atoms (10-Al, 10-O) is employed for ground state calculations. Along the z-axis, a large lattice vector of 20Å is chosen to avoid mirror image interaction. After getting ground state geometry, NH_3 and PH_3, respectively, are brought near the 2D surface, and allow the configuration to get relaxed within the DFT-based self-consistent field. Interaction with the surface is further explored by investigating structural and electronic changes. All calculations have been performed in the framework of density functional theory (DFT) using Troullier Martins's norm-conserving pseudo-potential [25]. The valence electrons are defined with double zeta double polarized (DZDP) basis set. The exchange-correlation part of hamiltonian has opted for generalized gradient approximation (GGA) in the form of Perdew, Burke, and Ernzerhof (PBE) [26]. An energy cutoff of 250Ry in the real-space grid is employed for numerical integration, and the choice for sampling k-point in the Brillouin zone is 9x9x1 using Monkhorst–Pack scheme [27]. The conjugate gradient algorithm has been used for lattice vectors and atomic position optimization. The Spanish initiative for electronic simulations with thousands of atoms (SIESTA) quantum chemical package [28] is used for all geometrical and structural investigations.

STRUCTURAL AND ELECTRONIC PROPERTIES

Structural Properties

The optimized geometry of Al_2O_3 is displayed in Fig.1, the in-planner atomic configuration has an average Al-N bond length of 1.69eV as reported before [15]. In the previous report, the stability of the 2D sheet (or monolayer) is predicted through phonon calculation. Therefore, we are confirmed with the ground state stability of the obtained optimized geometry in the present calculation. The pristine Al_2O_3 nanosheet has been further exploited to examine the adsorption of NH_3 and PH_3 on its surface, respectively. Al_2O_3 crystal has an ionic Al-O bonding with Al and O as electron-deficient and electron-rich centers, respectively. We are anticipating a similar bonding pattern in our calculation, hence, expect the electron-rich center of NH_3 and PH_3 to interact with the electron-deficient site (Al) as stated above. The present investigation reveals NH_3 and PH_3 interact with the surface of the Al_2O_3-nanosheet through distances of 2.12Å and 2.51Å, respectively. The toxic molecules are directed towards the 2D surface with lone pairs on respective pentavalent atoms (N and P). The closest atoms between the two fragments within NH_3-Al_2O_3 and PH_3-Al_2O_3 configuration are N, Al, P, and Al, respectively, as shown in Fig. 2a and 2b. Different orientations of the XH_3(X = N or P) molecule were relaxed on the Al_2O_3 monolayer and subsequent findings through formation energy calculation favored the depicted configuration of Fig. 2. Formation energy for NH_3/PH_3-Al_2O_3 is evaluated as

$$E_{Formation} = E_{XH_3-Al_2O_3} - (E_{Al_2O_3} - E_{XH_3}) \quad (1)$$

$E_{XH_3-Al_2O_3}$ $E_{XH_3-Al_2O_3}$, $E_{Al_2O_3}$ $E_{Al_2O_3}$ and E_{XH_3} E_{XH_3} are the total energy of XH_3-Al_2O_3, Al_2O_3-nanosheet and XH_3 molecule, respectively (where, X = N or P). The respective interactions of NH_3 and PH_3 are -1.41eV and -0.70eV, suggesting strong interaction with the monoatomic layer. With these findings, we are confident that a substantial change in an electronic configuration has taken place. This will be explored next through the partial density of state (PDOS) and band structure analysis.

Electronic Properties

Energy band structure analysis suggests the Al_2O_3 monolayer has an energy bandgap of 4.45eV (Fig. 3a), hence falling in the range of wide bandgap semiconductors. It is a direct bandgap semiconductor with conduction band minima (CBM) and valence band maxima (VBM) lying at Γ-point in k-space. A closed look at the energy band dispersion of the Al_2O_3-sheet reveals the flattening of energy band spectra after NH_3/ PH_3 interaction (Fig. 4 a) and (b). As band curvature

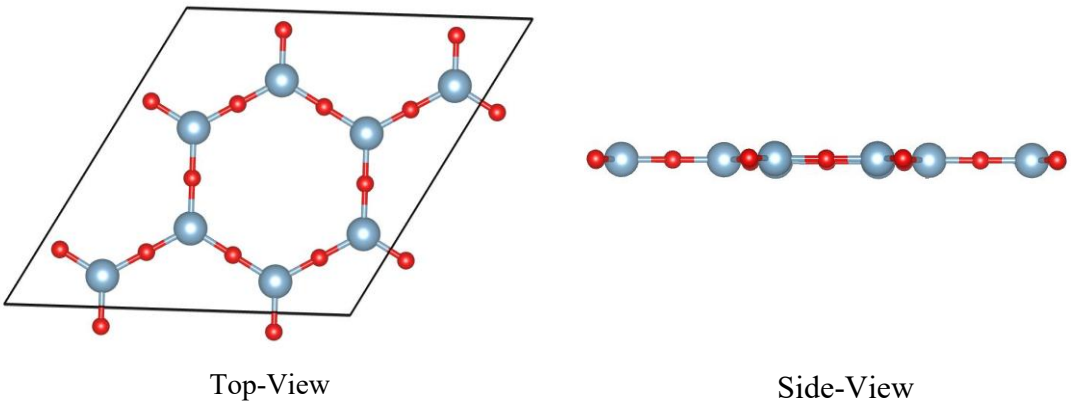

Fig. 1. Optimized ground state geometry of Al_2O_3 monolayer

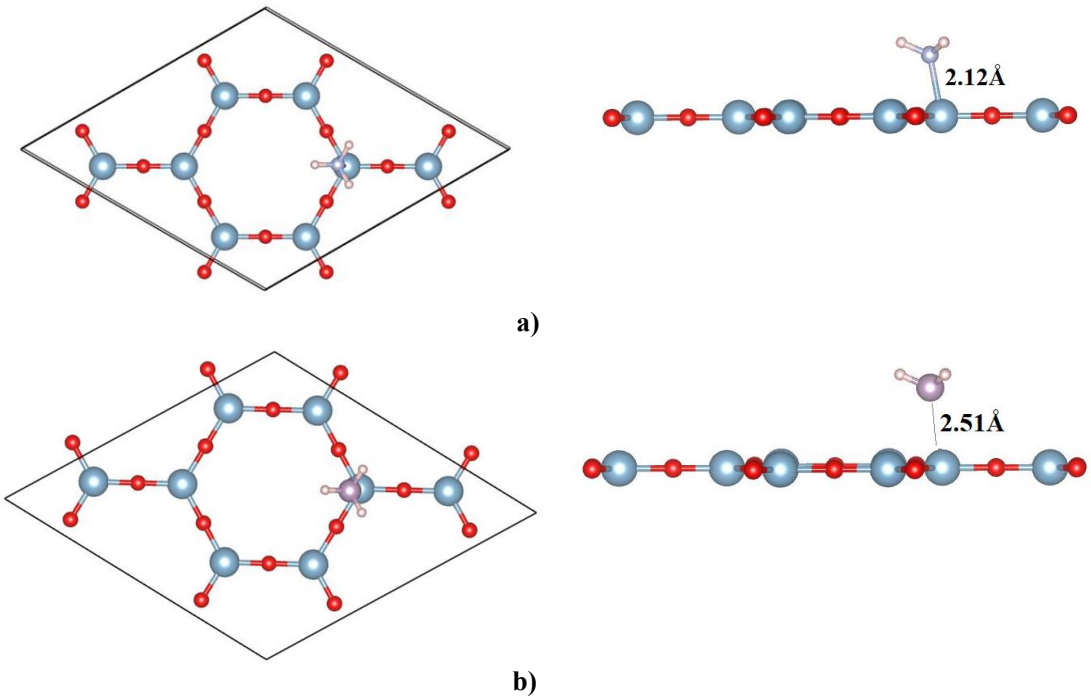

Fig. 2. Top and side-view of a) NH_3-Al_2O_3 and b) PH_3-Al_2O_3 atomic configuration.

is inversely proportional to the effective mass of the charge carrier, we expect the charge carrier (electron/hole) mobility of the 2D sheet will become sluggish after NH_3/ PH_3 adsorption. A slight reduction in the forbidden gap is observed for the molecularly adsorbed 2D sheets. A bandgap of 4.19eV ad 4.24eV is witnessed for NH_3-Al_2O_3 and PH_3-Al_2O_3 sheets, respectively. The holding of NH_3/PH_3 over the surface has further been confirmed through electronic charge transfer analysis. Mulliken population analysis identified a 0.42e charge transferred from NH_3 to the Al_2O_3 sheet. The charge contribution is mainly attributed to the electronic charge transfer from the lone pair of N to the p-orbitals of Al. A similar pattern is observed for PH_3-Al_2O_3 configurations with an electronic charge transfer of 0.33e. In Table.1, we have depicted important electronic and structural parameters to scrutinize the NH_3/ PH_3-Al_2O_3 monolayers. The role of inter-frontier orbital is very important in deciding the chemical behavior of an atomic configuration. In the present investigation,

Table. 1. Important parameters for studying the interaction properties of NH_3 and PH_3 on Al_2O_3-monolayers.

Configuration	Mulliken Charge Transfer (in e^-)	Energy gap E_g (in eV)	NH_3/PH_3 Distance (from the Al_2O_3 surface)	Formation energy (in eV) $E_{Formation}$
NH_3- Al_2O_3 monolayers	0.42	4.24eV	2.12Å	-1.41eV
PH_3- Al_2O_3 monolayers	0.33	4.19eV	2.51Å	-0.70eV

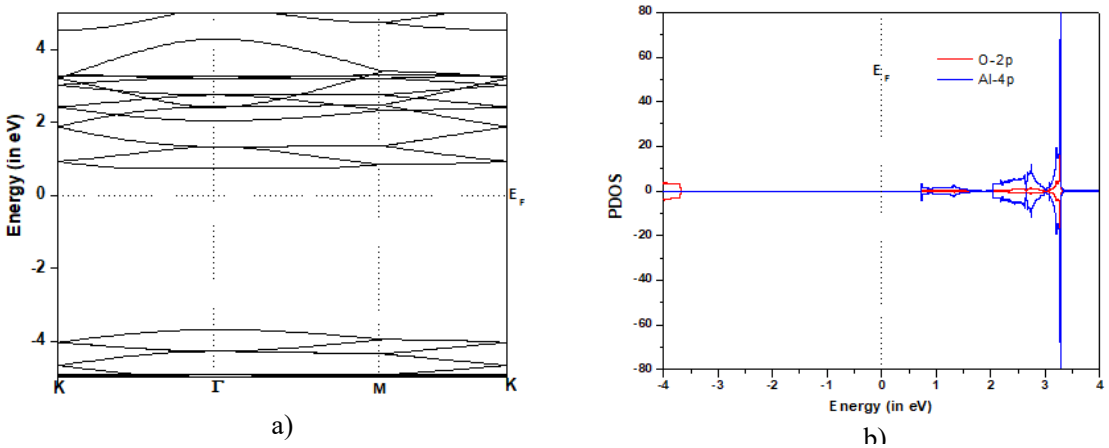

Fig. 3. a) Bandstrucutre and b) PDOS of pristine Al_2O_3 nanosheet

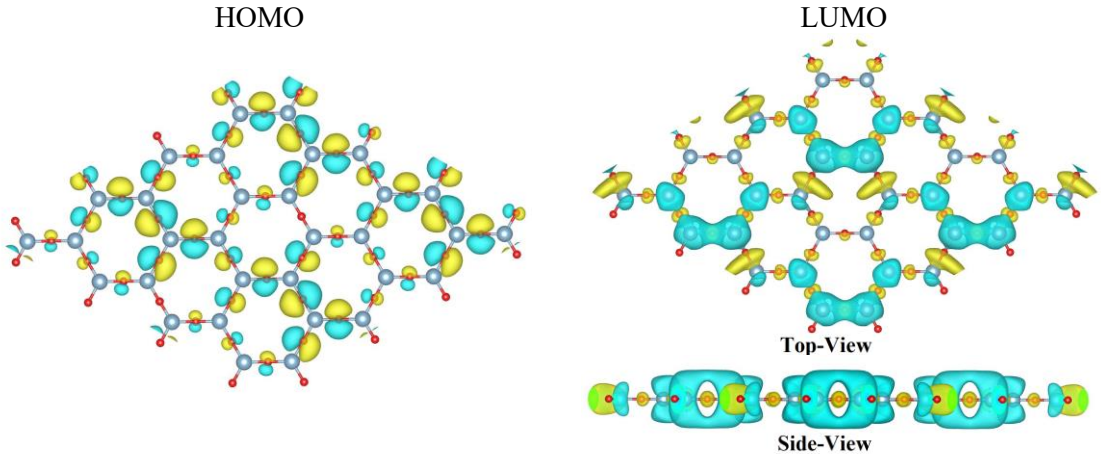

Fig. 4. Contour plot for HOMO and LUMO of the pristine Al_2O_3 nanosheet

the highest occupied molecular orbital (HOMO) consists of the Al-3p state and the lowest unoccupied molecular orbital (LUMO) is derived from hybridized Al-3p and O-2p state, as evident from the contour plot (Fig. 4). The same is demonstrated in the PDOS plot of pristine Al_2O_3 (Fig. 3b), no state available is close to the Fermi level. This was also confirmed through band-dispersion analysis in a band structure study. To predict the interaction taking place between NH_3/PH_3 and the Al_2O_3-sheet, fragmented DOS is shown in Fig. 5 (b) and (d), respectively. The availability of NH_3/PH_3 and the Al_2O_3-DOS at the inter-frontier orbital region (Fig. 3b) and (3d) suggests robust hybridization between molecular orbital from NH_3/PH_3 and the Al_2O_3 sheet. The N/P-p_z orbital gets hybridized with the p_z orbital of Al which causes it to hold NH_3 and PH_3 over the 2D surface. The conductivity of Al_2O_3 upon interaction with NH_3/PH_3 could be

$$\sigma = Ke^{\frac{-E_g}{2K_BT}}\sigma = Ke^{\frac{-E_g}{2K_BT}} \quad (2)$$

ion

where K is the proportionality constant, E_g defines

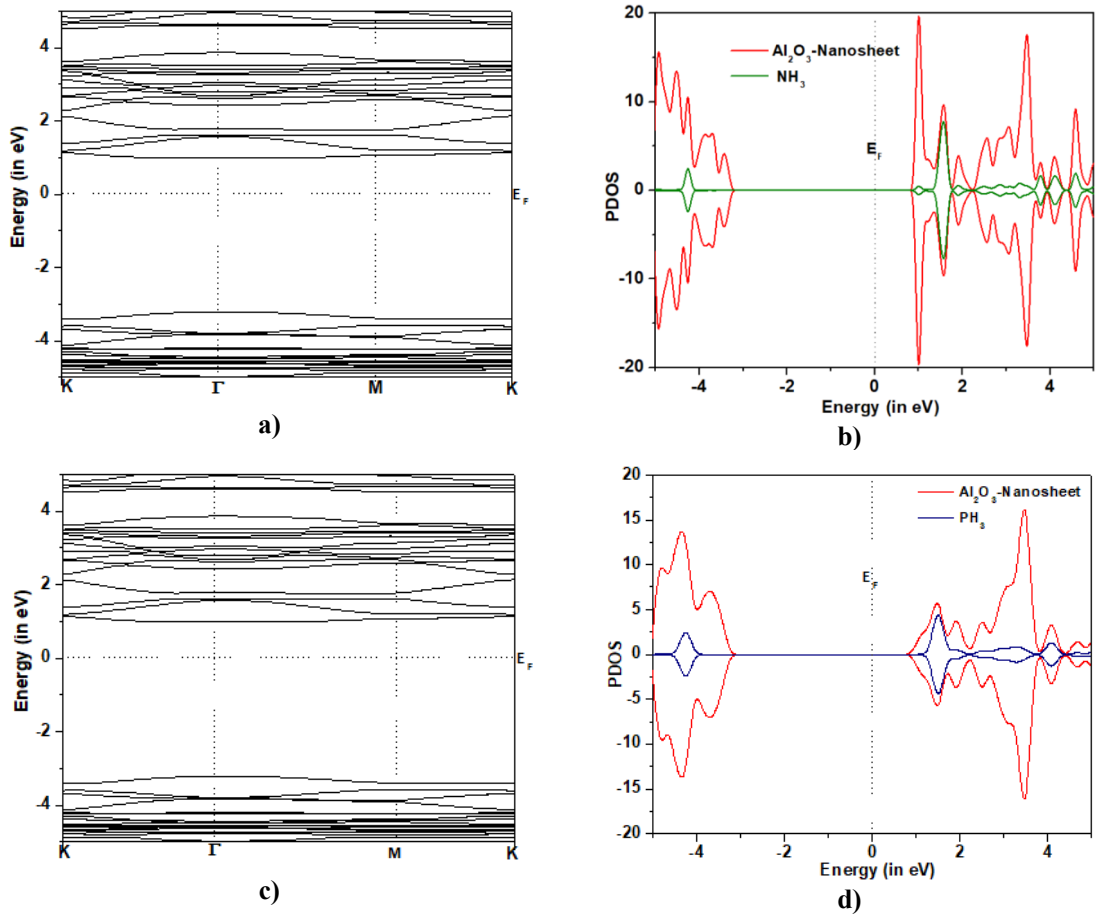

Figure. 5. Bandstructure and PDOS of a) NH_3-Al_2O_3 and b) PH_3-Al_2O_3.

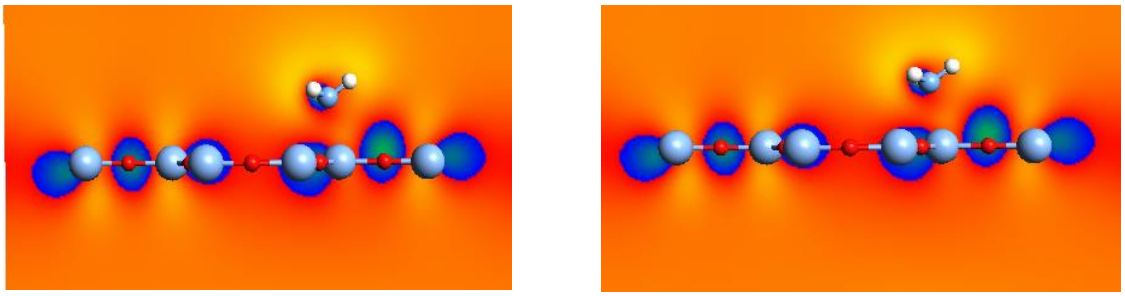

Figure. 6. Electrostatic potential difference contour plot of a) NH_3-Al_2O_3 and b) PH_3-Al_2O_3 nanosheet.

the energy bandgap, K_B is the Boltzmann constant and T is room temperature (300K).

As discussed above, NH_3/PH_3 interaction E_g decreased which signifies a rise in electrical conductivity. However, energy band flattening in the band structure diagram suggests increased effective mass of charge carriers, hence, decreased mobility. Thus, a competing condition is raised to determine the transport behavior of the NH_3/PH_3-Al_2O_3 nanosheet. The depiction of the electrostatic potential difference contour is shown in Fig. 3. The respective dark and light regions signify negative and positive charge accumulation. Relatively, more charge accumulation could be noticed between

NH_3 and the Al_2O_3 surface compared to the PH_3. Although the differences are very feeble as mentioned in Mulliken's population analysis, the contour plot depicts a localized charge pattern at O-atoms indicating ionic-bonding character within Al_2O_3-monolayer similar to the Al_2O_3-matrix.

CONCLUSIONS

In this work, we investigated the interaction pattern of NH_3/PH_3 towards the Al_2O_3-monolayer. The structural and electronic findings suggest a strong affinity of the toxic molecules towards the 2D nanosheet. With a binding strength of -1.41eV and -0.70eV the molecules were chemisorbed on the 2D surface. The 2D surface holds NH_3/ PH_3 at a distance of 2.12Å/2.51Å with 0.42e/0.33e charges transferred from the latter to the former. The electronic bandgap of the Al_2O_3-monolayer gets reduced by 0.26eV and 0.21eV, respectively, on interaction with NH_3 and PH_3. Envisaging inclusion of the toxic molecular state in the inter-frontier orbital region of the Al_2O_3-nanosheet is confirmed in our findings through PDOS analysis. Strong hybridization of lone pair orbital from NH_3/ PH_3 with the valence p-orbitals of O is the reason for electronic charge transfer between the two fragments. The conductivity equation and bandgap flattening indicate delicate competition in deciding charge transport characteristics of the NH_3/PH_3-Al_2O_3 configurations.

CONFLICT OF INTEREST

The authors declare no conflict of interest.

REFERENCES

1 C. Tan, X. Cao, X. J. Wu, Q. He, J. Yang, X. Zhang, H. Zhang, Recent advances in ultrathin two-dimensional nanomaterials. Chemical reviews, 117 (2017) 6225-6331. https://doi.org/10.1021/acs.chemrev.6b00558 https://doi.org/10.1021/acs.chemrev.6b00558

2 E. C. Anota, M. S. Villanueva, and H. H. Cocoletzi. "Density functional theory study of lithium and fluoride doped boron nitride sheet." Physica Status Solidi c 7 (2010) 2559-2561. https://doi.org/10.1002/pssc.200983909 https://doi.org/10.1002/pssc.200983909

3 N. D. Drummond, V. Zolyomi, and V. I. Fal'Ko. Electrically tunable band gap in silicene. Physical Review B 85 (2012) 075423. https://doi.org/prb/10.1103/PhysRevB.85.075423 https://doi.org/10.1103/PhysRevB.85.075423

4 P. Rani, G. S. Dubey, and V. K. Jindal. DFT study of optical properties of pure and doped graphene. Physica E: Low-dimensional Systems and Nanostructures 62 (2014) 28-35. https://doi.org/10.1016/j.physe.2014.04.010 https://doi.org/10.1016/j.physe.2014.04.010

5 P. Aghdasi, R. Ansari, Sh Yousefi, and M. Goli. Structural and mechanical properties of pristine and adsorbed puckered arsenene nanostructures: A DFT study. Superlattices and Microstructures 139 (2020) 106414. https://doi.org/10.1016/j.spmi.2020.106414 https://doi.org/10.1016/j.spmi.2020.106414

6 P. Aghdasi, S. Yousefi, and R. Ansari. Investigation of elastic properties, buckling and vibration of antimonene nanosheets through DFT-based finite element modeling. Materials Science and Engineering: B 271 (2021) 115219. https://doi.org/10.1016/j.mseb.2021.115219 https://doi.org/10.1016/j.mseb.2021.115219

7 P. Panigrahi, Y. Pal, T. Hussain, and R. Ahuja. "Application of germanene monolayers as efficient anchoring material to immobilize lithium polysulfides in Li-S batteries." Applied Surface Science 558 (2021) 149850. https://doi.org/10.1016/j.apsusc.2021.149850 https://doi.org/10.1016/j.apsusc.2021.149850

8 M. Rizvi, H. Gerengi, P. Gupta, Functionalization of Nanomaterials: Synthesis and Characterization. In Functionalized Nanomaterials for Corrosion Mitigation: Synthesis, Characterization, and Applications, American Chemical Society (2022)1-26. https://doi:10.1021/bk-2022-1418.ch001 https://doi.org/10.1021/bk-2022-1418.ch001

9 C. Dai, Y. Liu, D. Wei. Two-Dimensional Field-Effect Transistor Sensors: The Road toward Commercialization. Chemical Reviews 122 (2022) 10319-10392. https://doi.org/10.1021/acs.chemrev.1c00924 https://doi.org/10.1021/acs.chemrev.1c00924

10 M. S. Khan, M. S. Khan, Comparative theoretical study of iron and magnesium incorporated porphyrin induced carbon nanotubes and their interaction with hydrogen molecule. Physica E 44 (2012) 1857-186. https://doi.org/10.1016/j.physe.2012.05.010 https://doi.org/10.1016/j.physe.2012.05.010

11 Liu, Xianghong, Tiantian Ma, Nicola Pinna, and Jun Zhang. "Two- dimensional nanostructured materials for gas sensing." Advanced Functional Materials 27, (2017) 1702168. https://doi.org/10.1002/adfm.201702168 https://doi.org/10.1002/adfm.201702168

12 G. Neri. Thin 2D: The new dimensionality in gas sensing. Chemosensors 5 (2017) 21. https://doi.org/10.3390/chemosensors5030021 https://doi.org/10.3390/chemosensors5030021

13 H. Shahzad, R. Ahmadi, F. Adhami, J. Najafpour, Adsorption of Cytarabine on the Surface of Fullerene C20: A Comprehensive DFT Study. Eurasian Chemical Communication 2 (2020): 162-169. https://doi.org/10.33945/SAMI/ECC.2020.2.1 https://doi.org/10.33945/SAMI/ECC.2020.2.1

14 E.S. Mirkamali, R. Ahmadi, K. Kalateh, G. Zarei. Adsorption of Melphalan anticancer drug on the surface of carbon nanotube: A comprehensive DFT study. International Journal of New Chemistry. (2020).

15 T. T. Song, M. Yang, J. W. Chai, M. Callsen, J. Zhou, T. Yang, Z. Zhang, et al. The stability of aluminum oxide monolayer and its interface with two-dimensional materials. Scientific reports 6, (2016) 1-9. https://doi.org/nature.com/articles/srep29221 https://doi.org/10.1038/srep29221

16 N. Yamazoe, Toward innovations of gas sensor technology." Sensors and Actuators B: Chemical 108, no. 1-2 (2005) 2-14. https://doi.org/10.1016/j.snb.2004.12.075 https://doi.org/10.1016/j.snb.2004.12.075

17 M. S. Khan, A. Sriavstava. NH3 and NO2 adsorption analysis of GaN nanotube: A First principle investigation.

Journal of Electroanalytical Chemistry 775 (2016) 243-250. https://doi.org/10.1016/j.jelechem.2016.05.048 https://doi.org/10.1016/j.jelechem.2016.05.048

18 R. Ghosh, W. Julian W. Gardner, and Prasanta Kumar Guha. "Air pollution monitoring using near room temperature resistive gas sensors: A review." IEEE Transactions on Electron Devices 66, no. 8 (2019): 3254-3264. https://doi.org/ 10.1109/TED.2019.2924112 https://doi.org/10.1109/TED.2019.2924112

19 S. Kumar, V. Pavelyev, P. Mishra, N. Tripathi, P. Sharma, and F. Calle. A review on 2D transition metal di-chalcogenides and metal oxide nanostructures based NO2 gas sensors. Materials Science in Semiconductor Processing 107 (2020) 104865. https://doi.org/10.1016/j.mssp.2019.104865 https://doi.org/10.1016/j.mssp.2019.104865

20 T. R. Burns, M. L. Mace, S. D. Greenberg, and J. A. Jachimczyk. Ultrastructure of acute ammonia toxicity in the human lung. The American Journal of Forensic Medicine and Pathology 6, (1985) 204-210. https://doi.org/ DOI: 10.1097/00000433-198509000-00006 https://doi.org/10.1097/00000433-198509000-00006

21 A. Wang, Xi Zhang, H. Wang, and H. Xing. Recent evidence for toxic effects of NH3 exposure on lung injury: Protective effects of L-selenomethionine. Ecotoxicology and Environmental Safety 242 (2022) 113937. https://doi.org/ 10.1109/TED.2019.2924112 https://doi.org/10.1016/j.ecoenv.2022.113937

22 B. Berck, Sorption of phosphine by cereal products. Journal of agricultural and food chemistry 16 (1968) 419-425. https://doi.org/10.1021/jf60157a009 https://doi.org/10.1021/jf60157a009

23 M. S. Khan, A. Srivastava, R. Chaurasiya, M. S. Khan, and P. Dua. NH3 and PH3 adsorption through single-walled ZnS nanotube:Firstprincipleinsight.ChemicalPhysicsLetters636 (2015) 103-109. https://doi.org/10.1016/j.cplett.2015.07.038 https://doi.org/10.1016/j.cplett.2015.07.038

24 R. Bhuvaneswari, V. Nagarajan, and R. Chandiramouli. Arsenene nanoribbons for sensing NH3 and PH3 gas molecules-a first-principles perspective. Applied Surface Science 469 (2019) 173-180. https://doi.org/10.1016/j.apsusc.2018.11.003 https://doi.org/10.1016/j.apsusc.2018.11.003

25 N. Troullier, J. L. Martins. Efficient pseudopotentials for plane-wave calculations. Physical Review B 43 (1991) 1993. https://doi.org/10.1103/PhysRevB.43.1993 https://doi.org/10.1103/PhysRevB.43.1993

26 J. P. Perdew, K. Burke, M. Ernzerhof. Generalized gradient approximation made simple. Physical review letters 77 (1996) 3865. https://doi.org/10.1103/PhysRevLett.77.3865 https://doi.org/10.1103/PhysRevLett.77.3865

27 H. J. Monkhorst, J. D. Pack. Special points for Brillouin-zone integrations. Physical Review B 13, (1976) 5188. https://doi.org/10.1103/PhysRevB.13.5188 https://doi.org/10.1103/PhysRevB.13.5188

28 A. García, N. Papior, A. Akhtar, E. Artacho, V. Blum, E. Bosoni, P. Brandimarte, M. Brandbyge, J.I Cerdá, F. Corsetti, R. Cuadrado, V. Dikan, J. Ferrer, J. Gale, P. García-Fernández, V.M. García-Suárez, S. García, G. Huhs, S. Illera, R. Korytár, P. Koval, I. Lebedeva, L. P. López-Tarifa, S. G. Mayo, S. Mohr, Ordejón, Pablo; Postnikov, Andrei; Pouillon, Yann; Pruneda, Miguel; Robles, Roberto; Sánchez-Portal, Daniel; J. M. Soler, R. Ullah, V. Yu, Wen-zhe; Junquera, Javier (2020). Siesta: Recent developments and applications. Journal of Chemical Physics. 152 (20) 204108. https://doi.org/10.1063/5.0005077 https://doi.org/10.1063/5.0005077